



# Experimental and numerical investigations of $^{99}\text{TcO}_4^-$ diffusion in compacted SPV 200 bentonite

Yu-Hung Shih<sup>1</sup> · I-Hsien Lee<sup>2</sup> · Chuen-Fa Ni<sup>2,3</sup> · Tsuey-Lin Tsai<sup>1</sup> · Liang-Cheng Chen<sup>1</sup> · Chuan-Pin Lee<sup>4</sup> · Shih-Chin Tsai<sup>5</sup> · Te-Yen Su<sup>1</sup>

Received: 23 October 2017 / Published online: 23 March 2018  
© Akadémiai Kiadó, Budapest, Hungary 2018

## Abstract

Diffusion characteristics in bentonite are essential to quantify the transport of radionuclides through buffer/backfill materials in waste repositories. This study employs through-diffusion techniques to investigate the diffusion behavior of  $^{99}\text{TcO}_4^-$  through SPV bentonite with various densities. The apparent diffusion coefficients for bentonite densities are estimated using Marquardt–Levenberg optimization algorithm in the HYDRUS-1D model. Based on the experimental and calculation results,  $^{99}\text{Tc}$  could be considered as non-sorbing radionuclides. The data obtained in this study provide a valuable reference for the safety assessment of waste repositories.

**Keywords** SPV bentonite · Through diffusion · Apparent diffusion coefficient ( $D_a$ ) · Distribution coefficient ( $K_d$ )

## Introduction

In Taiwan, the safe disposal of high-level radioactive waste (HLW) from three nuclear power plants is an issue of critical importance. A proposal for the geological disposal of high-level radioactive waste has been accepted, in accordance with other countries, such as Sweden, Finland, Japan, and France. In the 1980s, the Taiwan Power Company (TPC), the owner of the nuclear power plants, investigated the long-term deep geological disposal of

spent nuclear fuel (SNF) and planned to construct a geological repository to begin operations in 2055 [1].

Technetium-99 ( $^{99}\text{Tc}$ ) is a pure  $\beta$ -emitter ( $E_{\max} = 292$  keV) and one of the key radionuclides formed at a high fission yield of 6.06% from  $^{235}\text{U}$  and  $^{239}\text{Pu}$  in nuclear reactors (approximately 6.1%). The high mobility of these materials in the geological environment [2, 3] and its very long half-life ( $2.13 \times 10^5$  year) underline the importance of assessing the safety of geological repositories. The proposed geological disposal of SNFs in Taiwan is based on a multi-barrier repository system, comprising a natural barrier of host rock and its surroundings (e.g., aquifers and biospheres), as well as an engineered barrier system. Chemical transport through diffusion plays an important role in many geological processes and diffusion coefficients can be used to assist in the design and evaluation of waste containment barriers. The diffusion of radionuclides in bentonite is usually predominant by anions in an oxidizing aqueous environment. Bentonite is commonly used as buffer/backfill material in geological disposal repositories, due to its excellent swelling, good sorption capability, high cation exchangeability, and low permeability [4, 5]. The sorption characteristics of radionuclides on bentonite are important in the safety assessment of disposal repositories. This has prompted extensive research into the

✉ I-Hsien Lee  
ihsienlee@ncu.edu.tw

<sup>1</sup> Chemistry Division, Institute of Nuclear Energy Research, No. 1000, Wenhua Rd., Jiaan Village, Longtan District, Taoyuan City 32546, Taiwan

<sup>2</sup> Center for Environmental Studies, National Central University, No. 300, Zhongda Rd., Zhongli Dist., Taoyuan City 320, Taiwan

<sup>3</sup> Graduate Institute of Applied Geology, National Central University, No. 300, Zhongda Rd., Zhongli Dist., Taoyuan City 320, Taiwan

<sup>4</sup> Department of Earth Sciences, National Cheng Kung University, Tainan City No.1, University Road, 70101, Taiwan

<sup>5</sup> Nuclear Science and Technology Development Center, National Tsing Hua University, Hsinchu 30013, Taiwan

sorption and/or diffusion of  $^{99}\text{Tc}$  (or analogous Re) on bentonite [6–13].

The conventional approach to measuring the diffusion coefficient is the through-diffusion (TD) method. The TD method is also applicable to weakly and non-sorbing tracers [14]. The samples in the TD method are located between two “in” and “out” reservoirs. Continuous samplings from the out reservoirs can produce a series of concentration measurements that represent the temporal mechanism of diffusion processes in the tested samples. Estimations of the effective diffusion coefficient ( $D_e$ ) and capacity factor for geological material are main tasks to the TD method. Previous investigations have relied on an approximate analytical solution under the assumption that the concentrations in both reservoirs remain constant, thereby ensuring nearly steady-state diffusive flux across the sample. Such steady-state diffusive flux enables the graphical method to obtain apparent diffusion coefficient ( $D_a$ ) for the TD method [15]. The experiments for diffusion of  $^{99}\text{Tc}$  through SPV 200 bentonite using through-diffusion technique has been shown elsewhere [16, 17]. Recent advantages of numerical techniques have improved the efficiency and accuracy in estimating parameters in complex flow and transport problems [18]. The objective of this study is to investigate the diffusion behavior of  $^{99}\text{TcO}_4^-$  through SPV 200 bentonite with various bulk dry densities. The modified TD method is proposed and the HYDRUS-1D numerical model is used to estimate diffusion coefficients. This study estimates the  $D_a$  by considering diffusion-dominated solute transport using the HYDRUS-1D model and compares the estimated  $D_a$  with those obtained from the graphical method.

### Governing equations of solute transport

The one-dimensional transport of solute can be expressed by a non-linear partial differential equation. The diffusion of solute in homogeneous porous media is usually solved by the form expressed as

$$\frac{\partial \theta_w C}{\partial t} = \frac{\partial}{\partial x} \left( \theta_w D \frac{\partial C}{\partial x} - qC \right) \quad (1)$$

where  $C$  is solute concentration associated with the solution,  $D$  is the dispersion coefficient of solute ( $\text{m}^2\text{s}^{-1}$ ),  $q$  is the volumetric fluid flux density of water ( $\text{ms}^{-1}$ ), and  $\theta_w$  is the volumetric water content ( $\text{m}^3\text{m}^{-3}$ ) ( $=\theta S$ ) porosity ( $\text{m}^3\text{m}^{-3}$ ),  $S$  is degree of saturation of water ( $\text{m}^3\text{m}^{-3}$ ). Under saturated flow conditions ( $S = 1$ ), the volumetric water content ( $\theta_w$ ) is equal to porosity ( $\theta$ ). The dispersion coefficient defined in a one-dimensional system attains the form,

$$D = D_a + \lambda v = D_a + \lambda \frac{q}{\theta_w} \quad (2)$$

where  $D_a$  is apparent diffusion coefficient ( $\text{m}^2\text{s}^{-1}$ ) in free water,  $\lambda$  is the dispersivity (m), and  $v$  is the average pore velocity ( $\text{ms}^{-1}$ ).

In this study, the through-diffusion experiments were designed under the saturated and homogeneous media, no advective flow and diffusion only solute transport. If there is no water flow in this model ( $q = 0$ ) then the solute transport equation can be written as follows:

$$\frac{\partial C}{\partial t} = D_a \frac{\partial^2 C}{\partial x^2} \quad (3)$$

The initial and boundary conditions of the model are given by

$$\text{I.C. } C(x, 0) = 0, 0 < x < L$$

$$\text{B.C. } C(0, t) = C_0 = \text{constant}, x = 0; t > 0,$$

$$C(L, t) = 0, x = L; t > 0$$

### Root mean square error (RMSE)

The statistical approach involved the calculation of the root mean square error, defined as the following Eq. (4), is the standard deviation of residuals ( $\gamma$ ), whereas  $N$  is the number of observations. Residuals are a measure of how far from the predicted values ( $C^m$ ) to observed values ( $C^o$ ) are.

$$\text{RMSE} = \sqrt{\frac{\sum_i^N (\gamma_i)^2}{N}} \quad (4)$$

$$\gamma_i = C^m - C^o \quad (5)$$

### R-squared ( $R^2$ )

$R^2$  is a measure of how much of the variance in observed values ( $C^o$ ) by the predicted values ( $C^m$ ) and is defined as the following Eq. (6), whereas  $\bar{C}^o$  is the mean of the observed values and  $N$  is the number of observations.

$$R^2 = 1 - \frac{\sum_i^N (C^m - C^o)^2}{\sum_i^N (C^o - \bar{C}^o)^2} \quad (6)$$

## Experiments and parameter estimations

### Geological material, tracer standards, chemicals, and aqueous phase

The materials used in this study were SPV 200 Wyoming bentonite, supplied by Cetco Europe Ltd (formerly

Volclay). SPV 200 bentonite originates in Lovell, Wyoming, USA. It is mainly composed of well-ordered sodium montmorillonite with minor quartz and cristobolite impurities. The SPV 200 is sodium (Na) bentonite with particles finer than 0.074 mm (U.S. mesh No. 200). The true density ( $\rho_t$ ) of the SPV 200 bentonite was  $2.68 \text{ g cm}^{-3}$ . Table 1 lists the average chemical composition of the synthetic underground water (SGW), representative of water sampled from six boreholes located at a depth of 400–500 m at a test site with crystalline rock in Taiwan. The ionic strength of groundwater in this area is in the range of 2.35–2.93 mM. The standard solution could be traceable to NIST SRM 4288A for  $^{99}\text{TcO}_4^-$ , respectively. The samples were measured using a liquid scintillation counter (LSC, Perkin Elmer Tri-Carb 3170 TR/SL) with counting efficiency of approximately 91% for  $^{99}\text{Tc}$ . The scintillation cocktail was Ultima Gold™ AB for  $^{99}\text{Tc}$ , respectively. 10 mL of the sample was placed in a 20 mL polyethylene counting vial followed by the addition of 10 mL of scintillation cocktail. All chemical reagents used in the experiments were of analytical purity and deionized water (DIW) was used in all experiments.

## Characterization

The specific surface area and chemical composition of SPV 200 bentonite were respectively analyzed using the  $\text{N}_2$ -BET measurement instrument (Micromeritics ASAP 2020) and wavelength dispersive X-ray fluorescence (WD-XRF) spectrometer (Kxios, PANalytical Inc). The mineralogical composition of the bentonite was determined by X-ray powder diffraction (XRD, D8 Advance, Bruker) under 40 kV and 40 mA with a ceramic Cu X-ray ( $\lambda = 0.15418 \text{ nm}$ ) tube.  $2\theta$ -scanning was conducted in the range of 5–80° at a rate of 1°/min. We employed a Lynx EYE compound silicon strip detector with lower

background ( $< 0.1 \text{ cps}$ ) and identified patterns via comparisons with JCPD standards.

## Through-diffusion experiment with constant concentrations in reservoirs

Bentonite clay samples with various dry densities (1.2, 1.4, 1.6, 1.8, and  $2.0 \text{ g cm}^{-3}$ ) were statically compacted using a lifting jack to form thin slabs of 3 mm in thickness with a cross-sectional area of  $19.6 \text{ cm}^2$ . The slabs were placed between two columns filled with SGW (100 mL), with the sample discs sandwiched between the source (inlet) and collection (outlet) reservoirs. The column units (reservoirs) were made of chemically inert polypropylene (PP) and one of the columns contained the diffusing radionuclide. Figure 1 presents a schematic drawing showing the column units used in the through-diffusion experiments. The sample was fixed using two Teflon O-ring washers (2.0 cm in height; 5 cm in diameter and 2.9 cm in thickness) and two porous filters (5 cm in diameter and 0.7 cm in thickness) with reinforced PP material at both ends of inlet and outlet reservoirs. Then, the sample holder was firmly fastened and tightly fitted with PP and screw-threads chamber units by an open wrench to reduce cell deformation, minimize diffusion resistance, and withstand swelling pressure induced by the bentonite clay upon saturation with water. Thus, the force due to strong swelling of bentonite was directly transmitted to the thick Teflon O-ring washers and porous filters, and then to the stiff structure (rigid PP diffusion cells). A commercially available micro-porous PVC-SiO<sub>2</sub> membrane (separator) with 40–50 nm pore size (Europe Amer-Sil™) was used to prevent the generation of colloids from the bentonite. The colloidal particles in aqueous suspension have an average size of 300 nm using laser diffraction particle size analyzers (Beckman Coulter, LS 230). H<sub>2</sub>O molecules of 2.75 Å and molecules of 5.04 Å were able to penetrate the membrane easily.

The procedures used in the through-diffusion experiment were as follows: (i) Before being poured into the source reservoir, the SGW underwent equilibration with the solid phase of compacted bentonite over a period of approximately 2 weeks, wherein an air pump was used to create suction pressure of  $2\text{--}3 \text{ kg cm}^{-2}$  to enable the injection of a large volume of water into the source reservoir and thereby accelerate the saturation process; (ii) Following water saturation, a very small volume of tracer solution,  $^{99}\text{Tc}$  spiked SGW, was poured into the source reservoir and maintained at a constant concentration of approximately  $1180 \text{ dpm mL}^{-1}$ ; (iii) Liquid samples of 10 mL (initially devoid of radioisotopes) were collected from the reservoir outlets at specific intervals, during which the source tank underwent circulation for 30 min using a peristaltic pump; (iv) The activity concentration of  $^{99}\text{Tc}$

**Table 1** Chemical composition of synthetic groundwater used in this study

Composition	Synthetic groundwater (SGW) (mol/L)
$\text{Cl}^-$	$9.77 \times 10^{-4}$
$\text{SO}_4^{2-}$	$1.0 \times 10^{-4}$
$\text{Na}^+$	$1.57 \times 10^{-3}$
$\text{K}^+$	$9.22 \times 10^{-5}$
$\text{Ca}^{2+}$	$3.76 \times 10^{-4}$
$\text{Mg}^{2+}$	$6.38 \times 10^{-5}$
TDS (mg/L)	~ 220
pH	8.06
Eh (mV)	~ 400

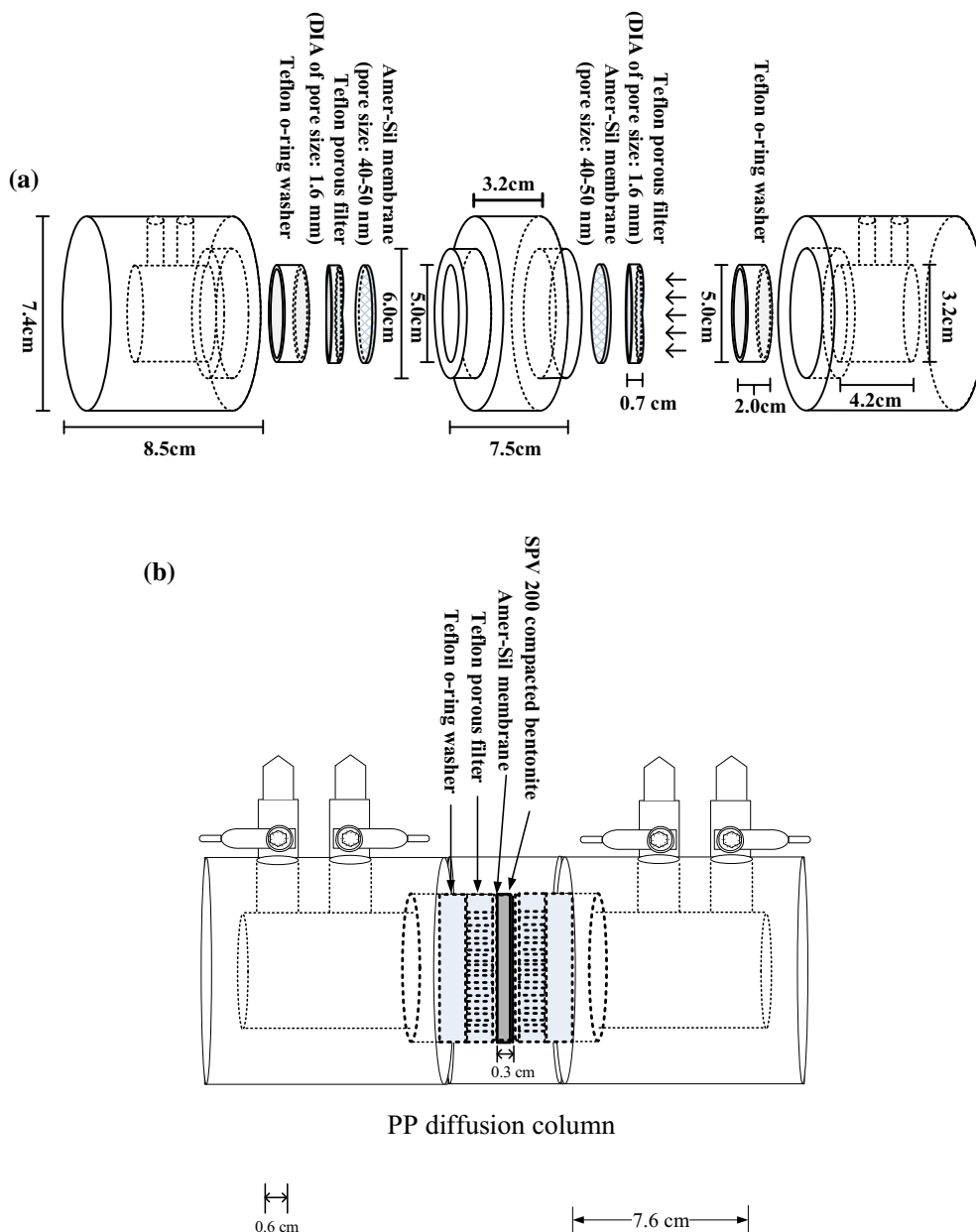


**Fig. 1** Schematic drawings showing diffusion column: **a** column unit, **b** after assembly

was determined using LSC; (v) Fig. 2 presents the experiment setup using five through-diffusion columns of various dry densities (1.2, 1.4, 1.6, 1.8, and 2.0 g cm<sup>-3</sup>).

During the experiment, the diffusion system was maintained at room temperature. The volume of the inlet reservoir was sufficient to keep the concentration at a near constant level (within a few percent) throughout the experiments. When the diffusion experiment was started, the solution in the collection reservoir was replaced with fresh solution (SGW) at regular time intervals (daily). The replaced solution was collected and measured using LSC to determine the activity concentrations of <sup>99</sup>Tc, which had

diffused out from the bentonite. Summing up the quantities of individual radionuclide in each collection reservoir and plotting the accumulated concentration ratio  $C_R(t)$  against the elapsed time  $t$  yielded the through-diffusion curves.

### Numerical model and parameter estimations

The HYDRUS-1D model is a one-dimensional finite element model for groundwater flow, multiple solutes, and heat transport in unsaturated–saturated media. The model solves the Richards' equation for water flow, Fickian-based advection dispersion equations for heat and solute transport

**Fig. 2** Experiment setup using five through-diffusion columns compacted to various dry densities (1.2, 1.4, 1.6, 1.8, and 2.0 g/cm<sup>3</sup>)

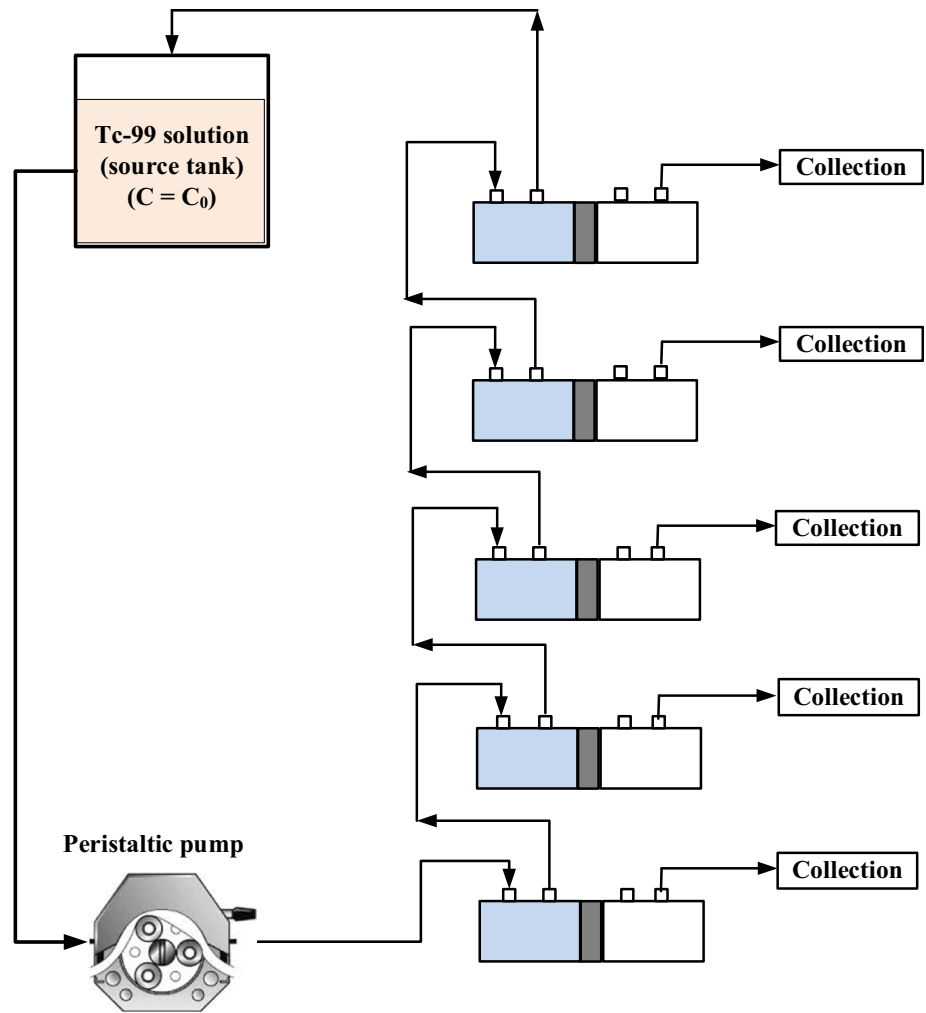


**Table 2** Diffusion parameters of <sup>99</sup>Tc in compacted SPV bentonite in SGW using experimental through-diffusion tests

Item	Sample no.				
	S 1.2	S 1.4	S 1.6	S 1.8	S 2.0
$\rho_b$ (g/cm <sup>3</sup> )	1.2	1.4	1.6	1.8	2.0
V (cm <sup>3</sup> )	86	85	87	88	84
$\theta$ (%)	56	48	40	33	25
$R_f$	1.00	1.01	1.02	1.01	1.06
$D_e$ (10 <sup>-12</sup> m <sup>2</sup> /s)	4.56 ± 3.0	2.56 ± 0.8	1.85 ± 0.9	1.40 ± 0.7	1.19 ± 0.1
$K_d$ (10 <sup>-3</sup> mL/g)	1.8 ± 0.1	3.6 ± 0.3	4.2 ± 1.4	6.0 ± 1.9	7.7 ± 2.1
$t_d$	0.95	0.61	0.51	0.49	0.52

$$\theta = 1 - \frac{\rho_b}{\rho_s}; R_f = D_e/\theta D_a; D_e = \frac{m \cdot V \cdot L}{A}; K_d = (R_f - 1) \theta / \rho_b; t_d = D_a^* t_f / L^2$$

and Marquardt–Levenberg type parameter estimation technique for inverse estimation of selected soil hydraulic and/or solute transport and reaction parameters [18]. Simulations of solute diffusion transport were carried out based on 0.3 cm bentonites with different densities of 1.2, 1.4, 1.6, 1.8, and 2.0 (g cm<sup>-3</sup>) using the HYDRUS-1D model. In this model, there were 1001 nodes applied to the

bentonite column, and the initial, minimum and maximum time steps were 0.001, 1 × 10<sup>-5</sup> and 5 days. Table 2 lists the porosity of each bentonite sample. The total simulation time is 12 days for all experimental cases. The concentration tolerance for model convergence is 1 × 10<sup>-5</sup> and the maximum number of iterations is 10 through the simulations. Based on the experiments that collect

**Table 3** The apparent diffusion coefficients obtained by model prediction and experimental data with  $R^2$

Density ( $\text{g cm}^{-3}$ )	Model prediction		Experimental data	
	$D_{a,\text{model}}$ ( $\text{m}^2\text{s}^{-1}$ )	$R^2_{\text{model}}$	$D_{a,\text{exp}}$ ( $\text{m}^2\text{s}^{-1}$ )	$R^2_{\text{exp}}$
1.2	$1.09 \times 10^{-11}$	0.9968	$(8.27 \pm 5.4) \times 10^{-12}$	0.9965
1.4	$4.66 \times 10^{-12}$	0.9952	$(5.27 \pm 1.7) \times 10^{-12}$	0.9217
1.6	$9.21 \times 10^{-12}$	0.9838	$(4.43 \pm 0.2) \times 10^{-12}$	0.9737
1.8	$5.22 \times 10^{-12}$	0.9947	$(4.22 \pm 0.8) \times 10^{-12}$	0.9000
2.0	$2.51 \times 10^{-12}$	0.9988	$(4.48 \pm 0.1) \times 10^{-12}$	0.9958

$$D_{a,\text{exp}} = \frac{L^2}{6t_x}$$

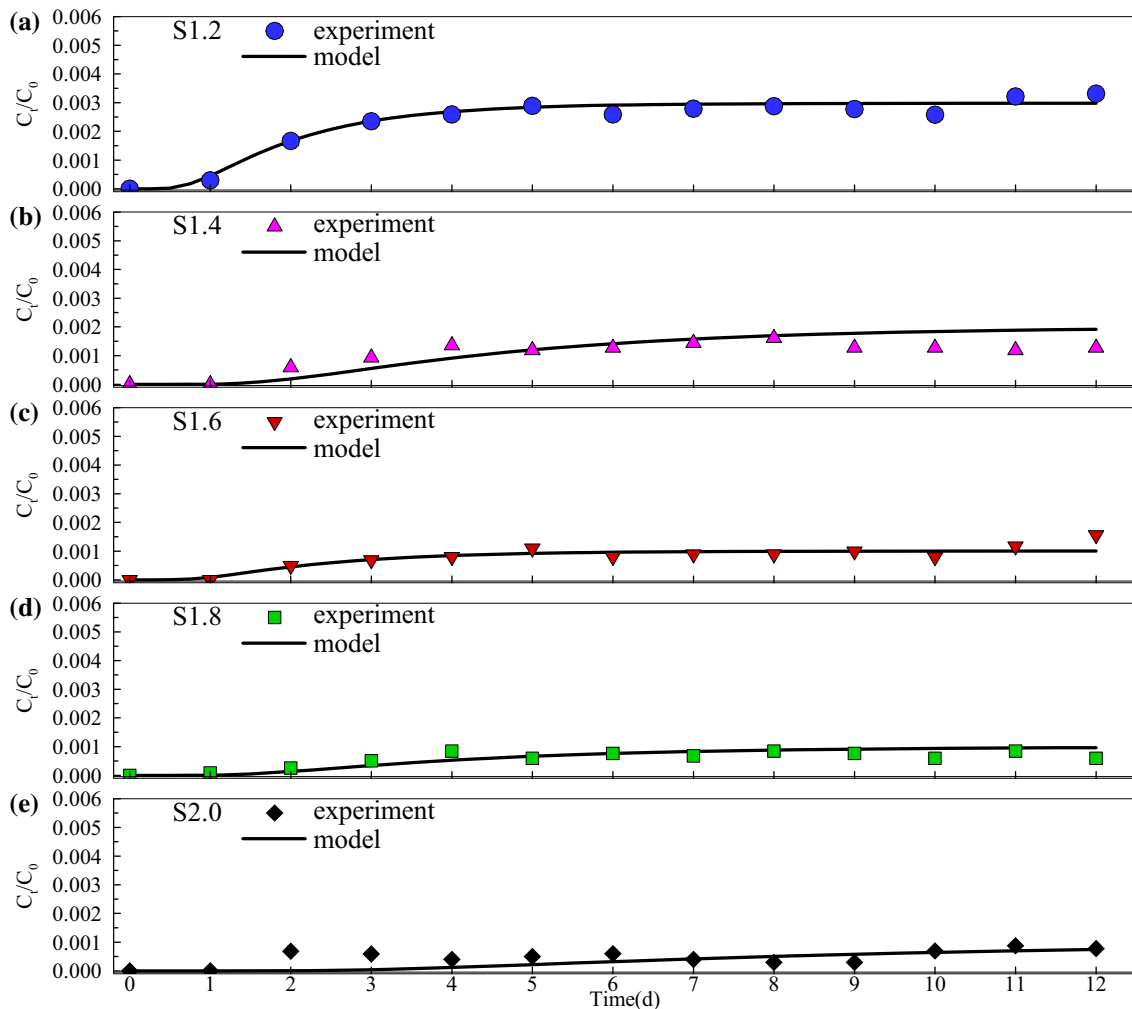


**Fig. 3** Breakthrough curves of  $^{99}\text{Tc}$  for experimental data (solid points) and simulation results (lines) in compacted bentonite with dry densities of 1.2, 1.4, 1.6, 1.8, and 2.0  $\text{g/cm}^3$

concentration at the outflow reservoir, the obtained concentration are the input data in the HYDRUS-1D for estimating  $D_a$  with different bentonite densities.

## Results and discussion

### Characterization

The  $\text{N}_2$ -BET surface area of the SPV 200 bentonite sample was  $29.8 \text{ m}^2/\text{g}$ . The chemical composition was determined

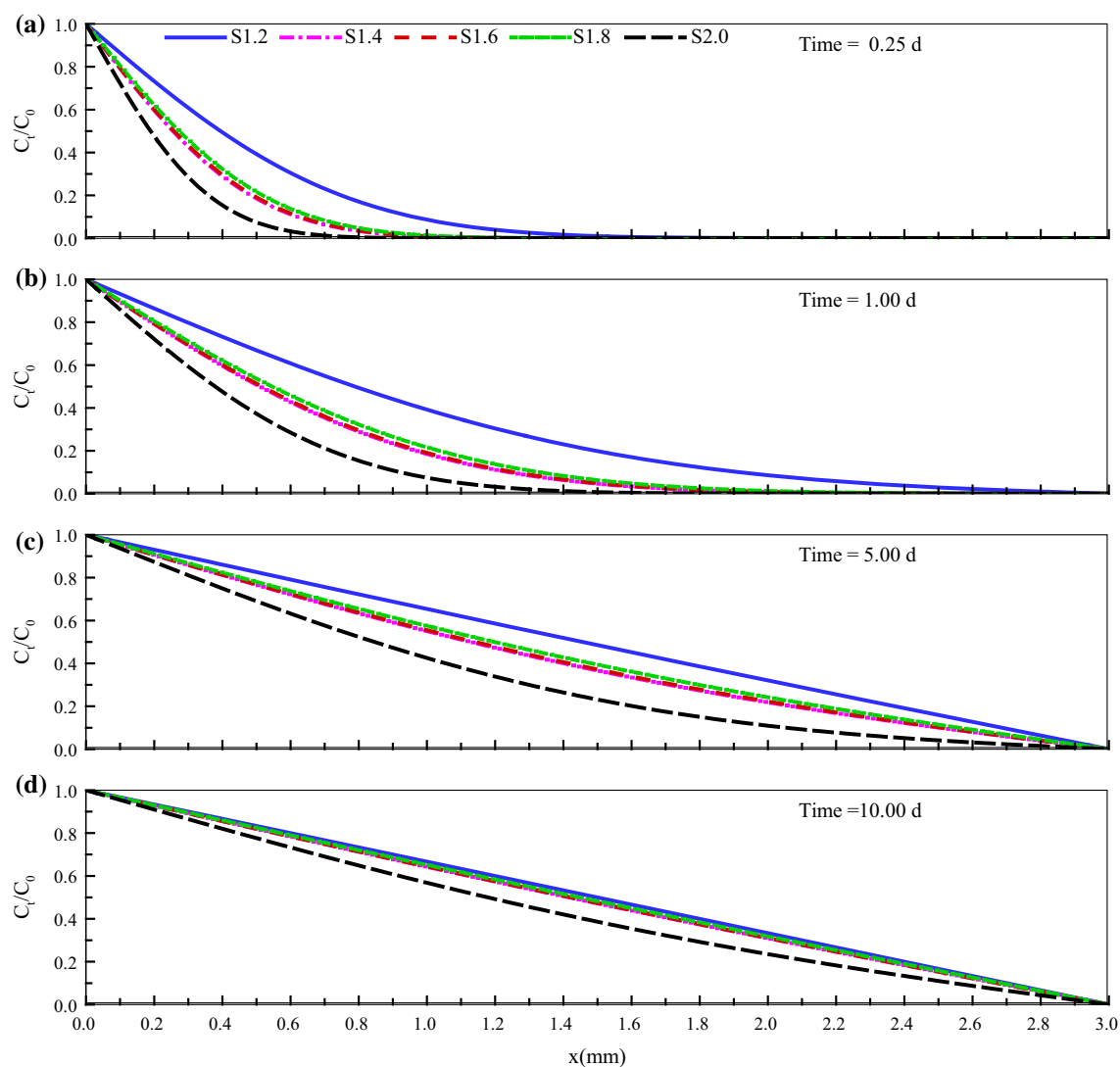


**Fig. 4** Concentration profiles versus length at **a** 0.25 day, **b** 1 day, **c** 5 day, and **d** 10 day for  $^{99}\text{Tc}$  transport in compacted bentonite

by XRF, as follows:  $\text{SiO}_2$  (58.89%),  $\text{Al}_2\text{O}_3$  (15.06%),  $\text{Fe}_2\text{O}_3$  (3.13%),  $\text{Na}_2\text{O}$  (2.20%),  $\text{CaO}$  (1.70%),  $\text{MgO}$  (1.59%),  $\text{K}_2\text{O}$  (0.59%),  $\text{TiO}_2$  (0.20%),  $\text{MnO}$  (0.08%),  $\text{P}_2\text{O}_5$  (0.07%),  $\text{LOI}$  (14.32%). The mineralogical analysis by XRD shows that the SPV bentonite are composed primarily of montmorillonite (81.4%), the main mineral phase and the other minerals contained in the bentonite are plagioclase (3.5%), muscovite (3.4%), quartz (3.0%), cristobalite ( $\sim 1\%$ ), tridymite (3.8%), illite (0.8%), gypsum ( $\sim 1\%$ ), pyrite (0.6%) and calcite (0.2%).

### Diffusion behavior of $^{99}\text{Tc}$ by experimental results

The apparent diffusion coefficient ( $D_a$ ), effective diffusion coefficient ( $D_e$ ), retardation factor ( $R_f$ ) and distribution coefficients ( $K_d$ ) were determined from the values of  $m$ ,  $V$ ,

$L$ ,  $A$ ,  $t_x$ ,  $\rho_b$ , and  $\theta$  [17]. The dimensionless parameter,  $t_d$  ( $t_d$  equals to  $\frac{D_a t_x}{L^2}$ ), is introduced here to determine whether the diffusion process reaches equilibrium. Crank [15] stated that steady state diffusion is achieved when  $t_d$  is larger than 0.45. Table 2 list the diffusion parameters of experiments involving compacted bentonite (0.3 cm slabs) of various densities. All of the  $t_d$  values for the  $^{99}\text{Tc}$  in each column exceeded 0.45, which suggests that the duration of the experiment was long enough to reach steady-state diffusion. The coefficients of the apparent and effective diffusion of  $^{99}\text{TcO}_4^-$  ranged from  $4.22 \times 10^{-12}$  to  $8.27 \times 10^{-12} \text{ m}^2 \text{ s}^{-1}$  and  $1.19 \times 10^{-12}$  to  $4.56 \times 10^{-12} \text{ m}^2 \text{ s}^{-1}$ , respectively. The distribution coefficients of  $^{99}\text{TcO}_4^-$  ranged from approximately 0.001 to  $0.0077 \text{ mL g}^{-1}$ , respectively. Our diffusion parameters are comparable to those obtained in previous studies [8, 9, 19, 20]. The differences between the values in this



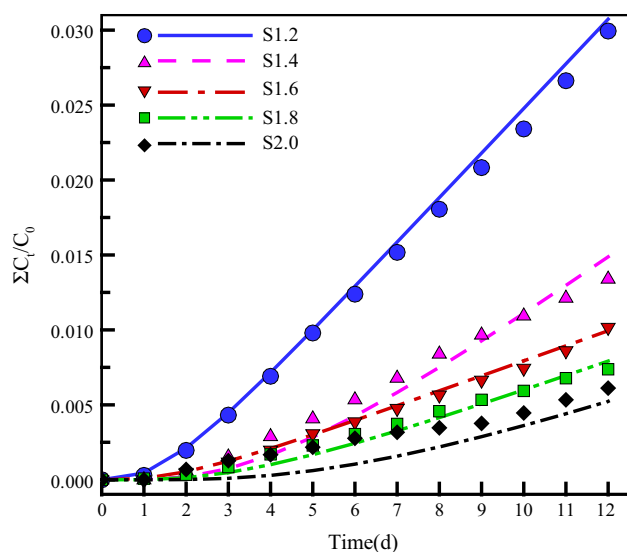


**Fig. 5** Accumulative break-through curves of  $^{99}\text{Tc}$  for experimental data (symbols) and modeling results (lines) in compacted bentonite with dry densities of 1.2, 1.4, 1.6, 1.8, and 2.0  $\text{g}/\text{cm}^3$

study and those in previous work can be attributed to differences in ionic strength and the pH value of the aqueous phase, the use of different types of bentonite. Most of the errors in the experiment data are due to the sampling process, measurements of radioactivity, and measurement of bentonite parameters.

As displayed in Table 2,  $^{99}\text{Tc}$  is heptavalent and anionic under oxidizing conditions, and exists as a negatively charged pertechnetate species [ $^{99}\text{Tc}(\text{VII})\text{O}_4^-$ ]. It is very poorly adsorbed on bentonite under these experimental conditions, due to the exclusion effect of bentonite associated with its negative surface charge. Diffusion experiments in this study were conducted under oxic conditions during operational phase. This is a conservative approach to the modeling of radionuclide transport behavior in the reducing environment commonly found in deep geological repositories. The very low diffusion coefficients may be attributed to high anionic exclusion effects in conjunction with the large size of the molecules.

### Simulation results and comparison with graphical method by experimental data

This study used HYDRUS-1D to estimate  $^{99}\text{Tc}$  diffusion coefficients for various densities of compacted bentonite samples. Table 3 shows similar results between the predicted and experimental data. HYDRUS-1D was used to optimize the diffusion coefficients with minimum values of RMSE by inverse estimation, from daily observation data. The fit of simulated diffusion coefficient to the observation data were obtained during the time-step concentration results of steady-state region, expressed as coefficient of

determination,  $R^2 > 0.98$ . Good estimation of the diffusion coefficient by graphical method requires that the diffusion process approaches a steady state. Similarly, the fit of calculated diffusion behavior to experimental data was found, represented as the coefficient of determination,  $R^2 > 0.90$ . It can also judge if the diffusion experiments have been performed sufficiently long to achieve a steady state. However, it may take several years to complete the diffusion experiment if the sample is fairly thick or highly-sorbing radionuclide. A numerical technique using the inverse method is proposed in this study to quickly determine the diffusion coefficient from all experimental data. Based on the daily observation data, the optimal values of the diffusion coefficients were computed using inverse estimation of HYDRUS-1D by achieving the minimum RMSE between measurement and simulation data, as shown in Fig. 3. According Table 3 and Fig. 3, the space-time distributions of solute concentration could be obtained by model prediction.

Figure 4 presents the concentration-depth profiles of  $^{99}\text{Tc}$  in the bentonite samples at times 0.25, 1, 5 and 10 days, respectively. The bentonite density of 1.2 ( $\text{g}/\text{cm}^3$ ) can lead to the fastest velocity of diffusive transport. However, the bentonite densities of 2.0 ( $\text{g}/\text{cm}^3$ ) presents the slowest diffusive transport (see Fig. 4). In Fig. 5, the daily cumulative concentration and the modeled cumulative concentration show consistently through the experimental processes. Although the diffusion coefficients can be easily obtained from the time-lag curve by fitting an asymptote in the steady-state part of the diffusion curve, the variations might come from the selection of steady-state regions on the diffusion break-through graphs, linear regression of the points along the line [21], and errors due to counting statistics (e.g., concentration of diffusing element, typically less than 5%). This is why the inverse modelling was used to verify the experimental results.

### Conclusions

The diffusion curves ( $\sum C_i/C_0$  over time) obtained through experiments in this study are consistent with theoretical breakthrough curves. The mathematical solution from Hydrus-1D model simulations of  $^{99}\text{TcO}_4^-$  diffusion in SPV 200 bentonite matched the observed data by graphical method. The simulation of  $D_a$  values under different densities of bentonite could be calculated at transient and steady-state by minimum RMSE and higher  $R^2$  could be also obtained at steady-state demonstrated the feasibility and reliability of using HYDRUS-1D. The apparent diffusion coefficients of technetium ranged from 4.22 to  $8.27 \times 10^{-12} \text{ m}^2 \text{ s}^{-1}$  and 2.51 to  $10.09 \times 10^{-12} \text{ m}^2 \text{ s}^{-1}$  for



through-diffusion tests and model prediction when the dry densities of compacted SPV 200 were in the range of 1.2–2.0 g cm<sup>-3</sup>. Under an oxidizing environment, technetium appears as a negatively charged pertechnetate species (<sup>99</sup>TcO<sub>4</sub><sup>-</sup>), which is poorly sorbed on bentonite ( $K_d < 0.01$  mL g<sup>-1</sup>) due to the anion exclusion effect associated with the negative surface charge of the bentonite particles. The diffusion coefficients obtained from the experimental results and model prediction could be used as input data for safety and performance assessment. SPV 200 bentonite could be considered as one of candidates for the buffer/backfill material aimed at radionuclide diffusion from high level nuclear waste.

**Acknowledgements** This work was financially supported by the Nuclear Backend Management Department at Taiwan Power Company.

## References

- Taiwan Power Company (2009) Preliminary technical feasibility study for final disposal of spent nuclear fuel—2009. Progress report
- Ikäheimonen TK, Vartti VP, Ilus E, Mattila J (2002) <sup>99</sup>Tc in Fucusand seawater samples in the Finnish coastal area of the Baltic Sea, 1999. *J Radioanal Nucl Chem* 252:309–313
- Chao JH, Tseng CL, Lee CL (2002) Sequential extraction separation for determination of <sup>99</sup>Tc in radwastes by ICP-MS. *J Radioanal Nucl Chem* 251:105–112
- Yu JW, Neretnieks I (1997) Diffusion and sorption properties of radionuclides in compacted bentonite, SKB TR 97-12. Svensk Kärnbränslehantering AB, Sweden
- Yang T, Knutsson S, Liu X (2016) Swelling properties and permeability of expandable clays of potential use for nuclear waste disposal. *J Earth Sci Geotech Eng* 6(2):9–61
- Zhao Y, Guo Z, Xu J (2013) <sup>99</sup>TcO<sub>4</sub><sup>-</sup> diffusion and sorption in compacted MX-80 bentonite studied by capillary method. *J Radioanal Nucl Chem* 298:147–152
- Liu DJ, Fan XH (2005) Adsorption behavior of <sup>99</sup>Tc on Fe, Fe<sub>2</sub>O<sub>3</sub> and Fe<sub>3</sub>O<sub>4</sub>. *J Radioanal Nucl Chem* 264:691–698
- Wang H, Wu T, Chen J, Fu BF, Zhao XH, Luo Y, Zhao YL, He CH (2015) Effect of humic acid contact time on the diffusion of Re(VII) in MX-80 bentonite. *Nucl Sci Tech* 26:S10314
- Xiao GP, Wu T, Wang H, Zheng Q, Zhang YJ, Pan GX, Shi L, Li JY (2015) Effect of inorganic salts on Se(IV) and Re(VII) diffusions in bentonite. *Nucl Sci Tech* 26:0503021–0503025
- Višňová H, Věčerník P, Jedináková-Řízková V (2006) Sorption characteristics of <sup>99</sup>Tc onto bentonite material with different additives under anaerobic conditions. *Radiochim Acta* 94:435–440
- Wang X, Tao Z (2004) Diffusion of <sup>99</sup>TcO<sub>4</sub><sup>-</sup> in compacted bentonite: effect of pH, concentration, density and contact time. *J Radioanal Nucl Chem* 260:305–309
- Wang H, Wu T, Chen J, Fu BF, Luo Y, Zhao Y, He CH (2015) Effect of humic acid on the diffusion of ReO<sub>4</sub><sup>-</sup> in GMZ bentonite. *J Radioanal Nucl Chem* 303:187–191
- Paul C (1997) Compilation of radionuclide sorption coefficients for performance assessment. SKB R-97-13, Svensk Kärnbränslehantering AB, Sweden
- García-Gutiérrez M, Cormenzana JL, Missana T, Mingarro M, Molinero J (2006) Overview of laboratory methods employed for obtaining diffusion coefficients in FEBEX compacted bentonite. *J Iber Geol* 32(1):37–53
- Crank J (1975) *The mathematics of diffusion*, 2nd edn. Clarendon Press, Oxford
- Lee CP, Tsai SC, Jan YL, Wei YY, Teng SP, Hsu CN (2008) Sorption and diffusion of HTO and cesium in crushed granite compacted to different lengths. *J Radioanal Nucl Chem* 275:371–378
- Shih YH, Tsai TL, Chen LC, Su TY, Lee CP, Tsai SC (2017) Determination of sorption and diffusion parameters of <sup>99</sup>Tc in crushed granite using through-diffusion experiments. *J Radioanal Nucl Chem* 311:1111–1116
- Šimůnek J, van Genuchten MT (2008) Modeling nonequilibrium flow and transport with HYDRUS. *Vadose Zone J* 7:782–797
- Hedin Allan (2010) Data report for the safety assessment SR-Site, SKB TR 10-52, December 2010. Svensk Kärnbränslehantering AB, Sweden
- Li JY, Dai W, Xiao GP, Wang H, Zhang ZT, Wu T (2012) Pertechnetate diffusion in MX-80 bentonite. *J Radioanal Nucl Chem* 293:763–767
- Szántó Z, Svingor É, Molnár M, Palcsu L, Futó I, Szűcs Z (2002) Diffusion of <sup>3</sup>H, <sup>99</sup>Tc, <sup>125</sup>I, <sup>36</sup>Cl and <sup>85</sup>Sr in granite, concrete and bentonite. *J Radioanal Nucl Chem* 252:133–138